ApplicationNOTE

GAMRY INSTRUMENTS

Dye Solar Cells – Part 2: Impedance measurements

Purpose of This Note

This application note is part of a series concerning dye solar cells. Theory and various types of experiments are discussed which are helpful for characterizing solar cells.

Part 1 of this series discusses basic principles of dye solar cells, their setup, and underlying electrochemical mechanisms.

This application note is part 2 and deals with electrochemical impedance spectroscopy (EIS) measurements on dye solar cells. The effect of various parameters is shown by means of experiments. Different EIS models are discussed which can be used to analyze impedance spectra.

Theory

Impedance spectroscopy with dye solar cells

As discussed in Part 1, various electrochemical processes take place in a dye solar cell (DSC). By measuring the I-V curves, many important parameters such as short-circuit current I_{SC}, open-circuit potential (E_{OC}), Fill factor FF, or cell efficiency η can be determined.

EIS offers additional information about various parameters of a DSC. When performing an EIS experiment, a specific point of an I-V curve can be analyzed (see also Figure 1).

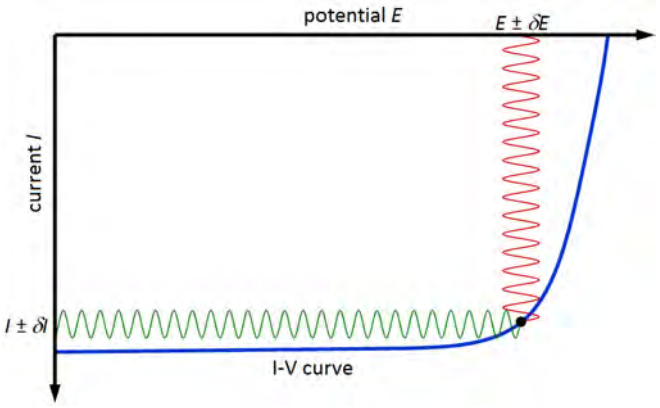

Figure 1 – Schematic outline of an impedance measurement with a DSC.

In this experiment, a DC-signal is applied to the cell which is superimposed by a small AC-signal ($E \pm \delta E$). The frequency of the sinusoidal signal is changed during the experiment and the current response of the cell is measured ($I \pm \delta I$). The sinusoidal signal has the same frequency as the applied signal but its phase is shifted. Both E and I are used to calculate the frequency-dependent impedance Z of the cell.

For detailed analysis, EIS models can be used to fit the measured curves. The next sections discuss various EIS experiments on DSCs and their analysis.

For more information on the theory of electrochemical impedance spectroscopy, see Gamry's application note at www.gamry.com:

Basics of Electrochemical Impedance Spectroscopy

Experiments

Figure 2 shows various Nyquist plots of a DSC at different potentials ranging from 0 V to 0.6 V. The applied AC-signal was 10 mV_{rms}. The frequency range was varied between 100 kHz and 10 mHz. During the experiment, a red LED (λ_{em} = 625 nm) was focused on the DSC with a constant intensity of about 24 mW.

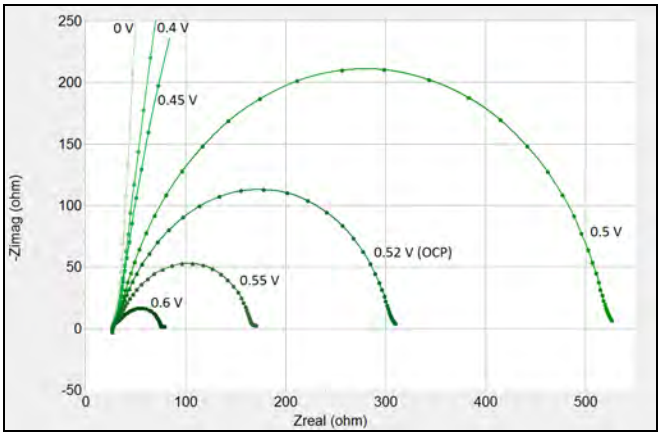

Figure 2 – Nyquist diagrams of a DSC at different potentials. For details, see text.

The shape of the Nyquist plots depends strongly on the applied potential. All curves exhibit a large arc at intermediate frequencies. The radius of the arc decreases with increasing potentials.

A small deformation can be observed at high frequencies (the left part of each curve). This semi-circle is nearly completely overlapped by the larger arc but it becomes more distinct at higher potentials.

Furthermore, an additional semi-circle appears at potentials above the open-circuit potential. Figure 3 shows an enlarged view of the Nyquist plot at 0.6 V.

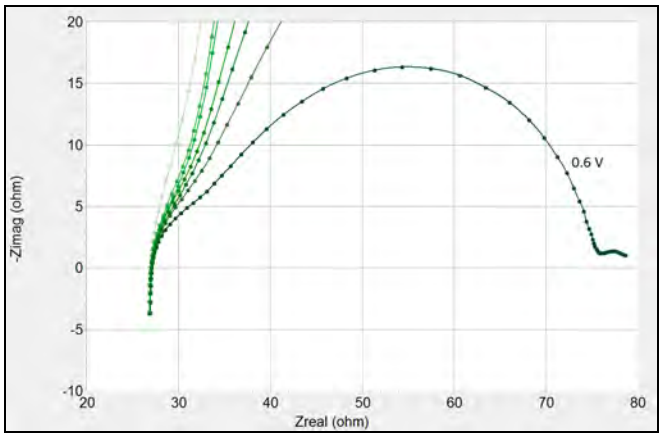

Figure 3 – Detailed illustration of the Nyquist diagram at 0.6 V.

The following sections introduce various EIS models that can be used to fit the Nyquist curves shown before. The fit results are used to describe the electrochemical system of a DSC for different potential regions more detailed.

Transmission line model

A specific type of EIS model is the transmission line. This model is often used when electrochemical systems with highly porous electrodes (e.g. TiO_2) are investigated. It takes the stepwise flux of ions within the pores of electrodes into account.

Gamry's Echem Analyst™ includes an editor which allows creating your own custom EIS models. In addition, various pre-built EIS models can be used instantly and modified if needed. One pre-built model is called *Unified* (Figure 4) and resembles a generic form of a transmission line.

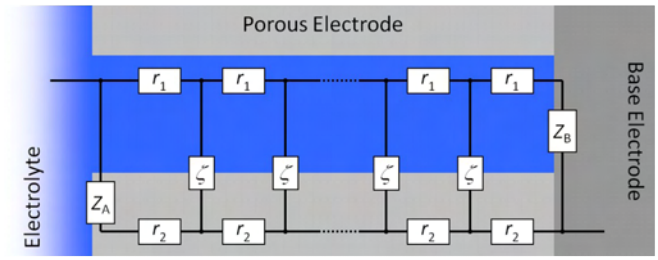

Figure 4 – Scheme of the *Unified* transmission line model. For details, see text.

The model consists of various components which are connected in series and parallel. The following components are used to describe the electrochemical system:

- Z_A Impedance at the outer surface of the electrode. Generally neglected because only reactions within the pore are taken into account ($Z_A = \infty$).
- Z_B Impedance at the back layer (substrate/electrolyte interface). Usually represented as parallel combination of a charge-transfer resistance (R_{BL}) and constant phase element (Q_{BL}) which describes a non-ideal double-layer capacitance.
- r_1 Distributed electrolyte resistance within a pore.
- r_2 Distributed resistance of the semiconductor.
- ζ Distributed impedance at the TiO_2/dye/electrolyte interface within the pore. Represented as a parallel combination of a transport resistance (r_ζ) and constant phase element (q_ζ).

For more information on transmission lines, see Gamry's application note at www.gamry.com:

Use of Transmission Lines for Electrochemical Impedance Spectroscopy

EIS models for different potential ranges

The *Unified* model shown in Figure 4 can be used to describe various cell conditions of a DSC by adjusting appropriate parameters.

In order to describe the Nyquist diagrams of a whole DSC, the *Unified* model is extended by three additional components:

- Z_{CE} Counter electrode impedance. Represented as a parallel combination of a charge-transfer resistance R_{CE} and a constant phase element Q_{CE}.
- R_S Series resistance. Represents the sum of bulk electrolyte, substrate, and electric contact resistances.
- W Porous bounded Warburg impedance. Also referred to as *open finite-length diffusion*.

Low potentials

As mentioned before, the shape of the Nyquist diagram of a DSC depends on the applied potential. At low potentials – which means near 0 V (short-circuit conditions) – the spectrum resembles a large arc (Figure 2).

We may assume that at very low potentials nearly no electrons are injected into the conduction band of the semiconductor because the band gap is too large. As a result, the distributed electrode resistance r_2 and the

impedance ζ of the TiO_2/dye/electrolyte interface are very high. Both elements thus may be neglected and the lower path of the transmission line drops out of the model. Instead, the main contribution to the measured impedance results from the back layer of the anode (Z_{BL}).

In addition, the electrolyte resistance r_1 within the pore can be neglected (r_1 is set to zero), for which we assume to be much smaller than r_2.

Further, we assume that most reactions occur within the pores because the electrode area within the pores is much higher compared to the outer surface of the electrode. As a result, Z_A is very high and it can be ignored.

The resulting EIS model for very low potentials is shown in Figure 5. Note that no distributed elements are used in contrast to the *Unified* model in Figure 4. The model does in this case not represent a transmission line.

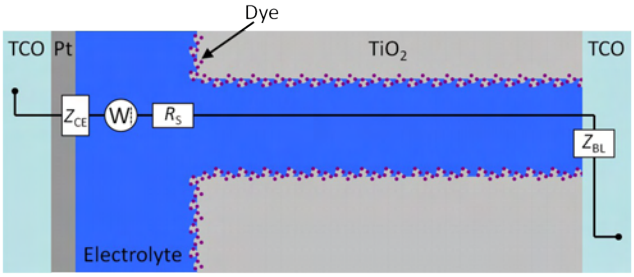

Figure 5 – EIS model of a DSC at low potentials near short-circuit conditions. For details, see text.

The small deformation of the Nyquist diagram (Figure 2) at very high frequencies can be assigned to the counter electrode impedance Z_{CE}. It is very small compared to the large semicircle resulting from the back layer impedance Z_{BL} which does nearly completely overlap the semicircle of the counter electrode.

The series resistance R_S shifts the whole Nyquist diagram to the right. It can be easily evaluated as the intersection between *x*-axis and Nyquist curve at high frequencies.

Diffusion may occur at these low potentials. However, it appears only at very low frequencies. This makes it impractical to be measured. Hence the diffusion contribution is ignored during fitting in this note.

Table 1 lists all parameters which were used to fit the Nyquist diagram at 0 V of Figure 2. Note that the constant phase element is described by an admittance parameter *Y* and a dimensionless exponent α.

R_{Pt} [Ω]	Y_{Pt} [S·s$^{\alpha}$]	α_{Pt}
3.16	$3.63 \cdot 10^{-6}$	1.0

R_S [Ω]
24.5

R_{BL} [Ω]	Y_{BL} [S·s$^{\alpha}$]	α_{BL}
$2.31 \cdot 10^{5}$	$4.10 \cdot 10^{-6}$	0.93

Table 1 – Parameters used to fit the Nyquist diagram at 0 V of Figure 2.

Intermediate potentials

The cell's electrochemical behavior changes at potentials below the open-circuit potentials. We can make some assumptions to build a suitable model for fitting.

The band gap of the semiconductor is now much smaller with increasing potentials. Electrons can be injected faster into the conduction band. As a result, the impedance ζ of the TiO_2/dye/electrolyte interface as well as the distributed electrode resistance r_2 decrease and need to be taken into account.

In contrast, the back layer impedance Z_{BL} is increasing and its influence to the total measured impedance is decreasing.

Again, we assume that the distributed electrolyte resistance r_1 is much smaller than the electrode resistance r_2. Hence r_1 can be set to zero or very small values. Reactions on the outer electrode surface can be ignored. We assume that Z_A is very high.

A schematic diagram of the EIS model for intermediate potentials is shown in Figure 6. Note that the model represents now a transmission line with distributed elements within the pore.

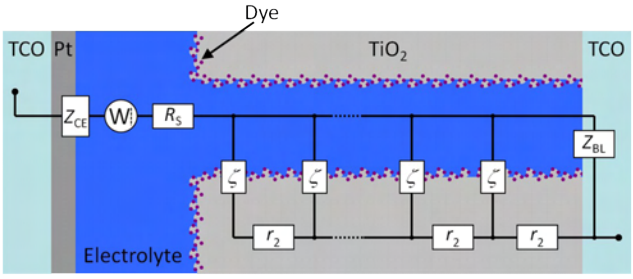

Figure 6 – EIS model of a DSC at intermediate potentials. For details, see text.

The Nyquist diagrams in this potential range (see also Figure 2) show that the contribution of the impedance at the counter electrode (Z_{CE}) is still small. It is still only visible as small deformation of the larger semicircle at intermediate frequencies.

The bigger arc which represents the complete transmission line becomes smaller with increasing potentials. Compared to the measurements at short-circuit conditions, reactions occur preferably along the electrode within the pore.

The Nyquist curves show at very low frequencies a small deformation. It indicates the diffusion processes but it can be still not clearly observed in this potential range. The diffusion element can be added during fitting. However, its fit parameters should be treated with caution. Much lower frequencies are needed in order to fit the diffusion element properly.

Table 2 lists all fit parameters for the Nyquist plot at 0.4 V in Figure 2. Z_A was fixed at a very high value during fitting and r_1 was set to a very low value. Note that the Warburg diffusion W is represented by an admittance parameter Y_W and a time constant B.

R_{Pt} [Ω]	Y_{Pt} [S·s$^{\alpha}$]	α_{Pt}
7.46	$5.04 \cdot 10^{-4}$	0.68

R_S [Ω]
26.3

Y_W [S·s$^{0.5}$]	B [s$^{0.5}$]
$1.36 \cdot 10^{-3}$	$6.75 \cdot 10^{-3}$

R_{BL} [Ω]	Y_{BL} [S·s$^{\alpha}$]	α_{BL}
$2.7 \cdot 10^{24}$	$6.88 \cdot 10^{-6}$	0.45

r_ζ [Ω]	Y_ζ [S·s$^{\alpha}$]	α_ζ
$8.75 \cdot 10^{-1}$	$4.88 \cdot 10^{-1}$	0.05

r_2 [Ω]
34.1

Table 2 – Parameters used to fit the Nyquist diagram at 0.4 V of Figure 2.

High potentials

Figure 3 shows the Nyquist diagram of a DSC at 0.6 V. At these high potentials (i.e. above the open-circuit potential), the high-frequency arc becomes more distinct. The radius of the second arc at intermediate frequencies decreases further. In addition, a third arc at low frequencies appears. Hence both former models can not be used anymore for fitting. In order to fit the curve, new assumptions are made to create a suitable EIS model.

The band gap between conduction band and non-conducting valence band decreases further when increasing the potential. As a result, the conductivity of the semiconductor increases and the electrode transport resistance r_2 may be ignored. The distributed resistance r_1 of the electrolyte within the pore is again ignored for which we assume to be much smaller than r_2.

Because both transport resistances (r_1 and r_2) are ignored, the distributed impedance ζ at the TiO_2/dye/electrolyte interface can be combined to a single element. It consists of a single charge-transport resistance R_{CT} in parallel to a constant phase element Q_{DL} representing a non-ideal double-layer capacitance.

We assume that both impedances Z_A and Z_{BL} are very high because most reactions occur at the TiO_2/dye/electrolyte interface within the pores. Their influence on the total impedance is very small and both parameters do not have to be considered in the EIS model.

Figure 7 shows the EIS model used to fit DSCs at high potentials. It fits very well the three arcs of the Nyquist diagram at 0.6 V shown in Figure 3.

Please note that similar to the experiments at very low potentials no distributed elements are used. The electrochemical behavior of the DSC at high potentials is described without using transmission lines.

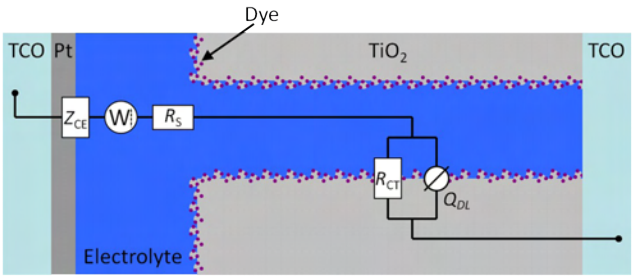

Figure 7 – EIS model of a DSC at high potentials. For details, see text.

The small overlapped arc at high frequencies can be again assigned to the impedance Z_{CE} of the counter electrode. The second arc at intermediate frequencies describes the electrochemical behavior at the TiO_2/dye/electrolyte within the pore (R_{CT} and Q_{DL}).

The third arc at low frequencies can be assigned to diffusion. It gets more distinct with increasing potentials. Its contribution to the total impedance can be now measured as it shifts to higher frequencies.

Table 3 lists all fit parameters which were used to model the Nyquist plot at 0.6 V of Figure 3.

R_{Pt} [Ω]	Y_{Pt} [S·s$^{\alpha}$]	α_{Pt}
7.65	$2.08 \cdot 10^{-5}$	0.82

R_S [Ω]
26.7

Y_W [S·s$^{0.5}$]	B [s$^{0.5}$]
$3.75 \cdot 10^{-1}$	1.17

R_{CT} [Ω]	Y_{DL} [S·s$^{\alpha}$]	α_{DL}
41.4	$5.28 \cdot 10^{-5}$	0.84

Table 3 - Parameters used to fit the Nyquist diagram at 0.6 V of Figure 3.

The fit results show that the series resistance R_S stays nearly constant at about 26 Ω within the entire potential range. The resistance R_{Pt} at the platinum counter electrode increases only a little.

In contrast, the resistance R_{BL} at the back layer of the anode increases drastically with increasing potentials. This trend is also in agreement with theory. The conduction band of the semiconductor decreases with increasing potentials resulting in higher impedances at the back layer.

Note also the difference between the distributed charge-transfer resistance r_ζ and the single resistance R_{CT}. The first parameter represents a resistance which is distributed along the inside of the pore. Its value depends also on the pore depth. R_{CT} represents the resistance of the entire inner electrode surface. Both values are difficult to compare.

Time constants

Figure 8 shows the corresponding Bode plots of the experiments shown above. The negative imaginary part of the impedance is plotted versus the frequency in a double-logarithmic style.

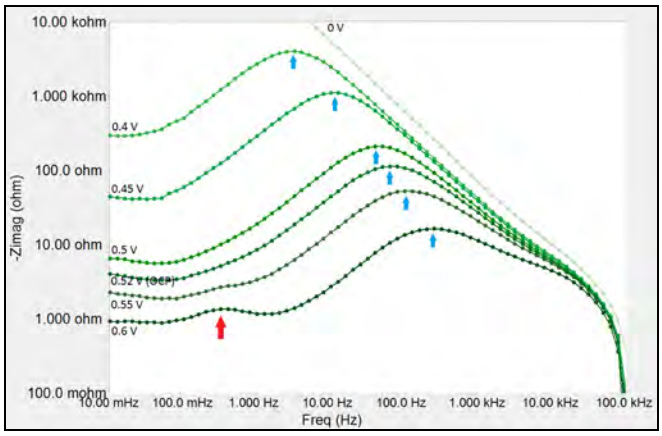

Figure 8 – Bode plots of $-Z_{imag}$ of a DSC at different potentials. For details, see text.

All curves exhibit local maxima at different frequencies f^*. The corresponding frequencies are related to time constants τ of various electrochemical phenomena by following equation.

$$\tau = \frac{1}{2\pi \cdot f^*}$$

The maximum at higher frequencies (indicated with blue arrows) corresponds to the charge-transfer at the TiO_2/dye/electrolyte interface. It shifts to higher frequencies with increasing potentials. The maximum shifts in this example from 3.2 Hz at 0.4 V to 252 Hz at 0.6 V. Hence the time constant decreases which means that the rate for the charge-transfer increases. Under short-circuit conditions (0 V), the maximum is at about 50 mHz. The time constant for the charge-transfer is very high at such low potentials.

This trend is also consistent with the data gained from the EIS measurements. Most reactions occur on the back layer of the electrode at short-circuit conditions. With increasing potentials, the band gap of the semiconductor decreases. Electron injection into the conduction band is favored over reactions at the back layer of the electrode. As a result, the time constant for the charge-transfer at the TiO_2/dye/electrolyte interface decreases with increasing potentials.

The second maximum (indicated with a red arrow) can in general only be observed at high potentials and low frequencies. The time constant corresponds to the diffusion process which is very slow. The maximum is at about 317 mHz for the measurement at 0.6 V.

The maximum shifts down to lower frequencies with decreasing potentials which makes it in general impractical to measure.

Summary

This application note covers EIS measurements with dye solar cells. Theory about electrochemical impedance measurements is addressed. Gamry's pre-built *Unified* transmission line model is shown and its various components are discussed.

In addition, theory is applied by means of EIS experiments on DSCs at different potentials. Nyquist plots are shown and their analysis is explained by using different EIS models.

Finally, it is discussed how time constants of various electrochemical processes can be determined by evaluating Bode diagrams.

C3 Prozess- und Analysentechnik GmbH
Peter-Henlein-Str. 20
85540 Haar b. München

Tel: 089/45600670
FAX: 089/45600680

info@c3-analysentechnik.de
www.c3-analysentechnik.de

www.gamry.com